Scientific Research Publishing

Materials Sciences and Applications, 2022, 13, 279-299
https://www.scirp.org/journal/msa
ISSN Online: 2153-1188
ISSN Print: 2153-117X

Characterization of Flaxseed Oil for Nuclear Magnetic Resonance and Its Encapsulation

Karoline Da Silva Santana, Maria Inês Bruno Tavares

Instituto de Macromoléculas Professora Eloisa Mano (IMA) da Universidade Federal do Rio de Janeiro, Centro de Tecnologia Ilha do Fundão, Rio de Janeiro, RJ, Brasil

Email: mibt@ima.ufrj.br

How to cite this paper: Santana, K.D.S. and Tavares, M.I.B. (2022) Characterization of Flaxseed Oil for Nuclear Magnetic Resonance and Its Encapsulation. *Materials Sciences and Applications*, **13**, 279-299.
https://doi.org/10.4236/msa.2022.135015

Received: February 19, 2022
Accepted: May 13, 2022
Published: May 16, 2022

Abstract

Flaxseed (*Linum usitatissimum L.*) is one of the oldest crops known by humans and it has been used in numerous applications, such as in the textile industry, feed formulation, fertilizers, and paper industry. However, nowadays these seeds have won an important highlight for human consumption due to their active ingredients that make them an excellent functional food. Thus, this study aimed to extract flaxseed oil, an oil rich in omega 3 and 6, characterize it by using nuclear magnetic resonance (NMR) and Fourier-transform infrared spectroscopy (FTIR) and then encapsulate this oil in polycaprolactone (PCL) on the micro scale, using the nanoprecipitation technique and subsequently freeze-drying. To determine the mean diameter, the dynamic light scattering technique (DLS) was used, and to verify whether there was encapsulation, the pulse sequence MSE-FID, an NMR sequence in the time domain, was also used. In addition to the previously mentioned techniques, X-ray diffraction (XRD) was also employed. Flaxseed flour was also analyzed by time-domain NMR and FTIR. The results obtained by NMR show that the oil consists of fatty acid esters in the form of triglycerides in which there is the presence of esters of α-linolenic and linoleic acids, respectively ALA and LA, according to the literature. Regarding the material after encapsulation, it presented a mean diameter of 445.2 ± 41 nm and PDI of 0.674 ± 0.064, therefore classified as microparticles. Finally, using the sequence MSE-FID and the FTIR, it can be concluded that there has been the microencapsulation of flaxseed oil in the particles formed.

Keywords

Flaxseed, NMR, Functional Food, Encapsulation

1. Introduction

Flaxseed is considered an important functional food because it has numerous

substances considered beneficial to health in addition to its nutritional value [1]. Flaxseeds are an excellent source of minerals, vitamins, proteins, and fatty acids, but the main substances present are fiber, lignans, and unsaturated fatty acids [1] [2].

Flaxseed oil is rich in essential fatty acids such as alpha-linolenic acid (ALA) and linolenic acid (LA) [3], therefore is considered the richest source of this type of oil, even presenting an excellent ratio of ω–6/ω–3 [2]. Fibers are made up of insoluble fibers, cellulose, hemicellulose, and lignans, while mucilage gum forms the soluble fiber fraction [1].

Flaxseeds are also known to contain the highest content of lignans [2]. Lignans act as antioxidants and phytoestrogens, and the most predominant is the secoisolariciresinol diglucoside (SDG) [4]. Due to the presence of these components, flaxseed has been related to the prevention or control of numerous diseases, such as cardiovascular diseases, cancer, obesity, diabetes, cholesterol control, blood glucose control, etc [5] [6] [7].

Another interesting study showed that the use of flaxseed enhanced the growth of *L. acidophilus* and improved its bile tolerance, which is an in vitro test that evaluates the ability of the strain to survive in a media with bile salts similar to human small intestines, this test is an important criterion for probiotics for incorporation into foods and beverages [8].

Thus, the frequent consumption of this functional food is important, whether in its fresh form or even incorporated into other foods such as bread, cookies, cakes, and dairy products [1]. Micro or nanoencapsulation can be used when it comes to the incorporation of substances in other foods in order to preserve the characteristics of the incorporated substance and mask the unpleasant taste in the final product [9] [10].

Nano or microencapsulation consists of wrapping bioactive in capsules in the micro or nano size range to protect them against deterioration caused by environmental conditions, such as high temperatures, oxygen, light, pH variations, and unwanted interactions with other substances, etc. [11]. In these formulations, the actives are involved by a material, or a combination of materials, and a series of techniques can be chosen depending on the desired system. Some techniques reported in the literature are spray drying, freeze-drying, emulsification, coacervation, and nanoprecipitation, among others [10] [12].

Nanoprecipitation was the technique used in this work, in this method, an organic solution containing the polymer and the active is emulsified in an aqueous solution (with or without surfactant). Then, the organic solvent is removed by stirring (with or without vacuum) and this process allows the formation of nanoparticles [13]. The basis of this technique involves an organic phase being added to the aqueous phase, the solvent phase tends to have a diffusion effect, while the polymer automatically tends to collapse forming the micro or nanoparticles that can encapsulate an active ingredient [14].

Although it is an easy-to-apply technique, a form of drying is needed after it is carried out, such as lyophilization, and only polymeric materials can be used as a

wall material [15].

In order to analyze the substances or materials obtained both in the extractions and after encapsulation, several techniques can be used, one of them is NMR.

NMR spectroscopy is mainly used to characterize liquid state samples, however, recent developments such as magic angle rotation (MAS), high-resolution magic angle rotation (HR-MAS), cross-polarization (CP), and cross-polarization with magic angle spinning (CP-MAS) opened new horizons for solid-state NMR experiments, so NMR can be used for both liquid and solid-state samples, in one-dimensional, two-dimensional and multidimensional experiments, providing information on structure, composition, purity, molecular weight, dynamics, and diffusion properties [16] using for this the magnetic properties of the analyzed nucleus.

In this way, the objective of this study was to extract, characterize and microencapsulate flaxseed oil in PCL using the nanoprecipitation technique. Moreover, TD-NMR was used to analyze the flaxseed flour obtained as extraction residue and the material after encapsulation, since it provides information on the structure and properties of the material, in addition to allowing a detailed study of the crystalline and amorphous domains [17].

2. Experimental

2.1. Materials

In this study, what were used are polycaprolactone (PCL) (Mn = 10,000 g/mol), Pluronic® F-68 (Mn = 8400 g/mol), acetone, ethanol, chloroform, and ethyl acetate P.A. All were obtained from Sigma-Aldrich®. Flaxseed oil was extracted in the laboratory.

2.2. Extraction of Flaxseed Oil

For the extraction of flaxseed oil, the Soxhlet method was used. The seeds were crushed with the aid of a blender, turning them into flour, and then 10 g of the flour was weighed and stored in a paper filter to be subsequently placed inside the Soxhlet extraction chamber. With the apparatus set up, the extractions were made with 10 cycles using ethanol, chloroform, and ethyl acetate/ethanol (3:1) in each extraction. In the end, the solvents were evaporated in a rotary evaporator.

2.3. Encapsulation of Flaxseed Oil

To carry out the encapsulation of flaxseed oil, it was necessary to prepare two solutions in advance, one being the aqueous phase and the other the organic phase. The aqueous phase contained 100 ml distilled water and 0.12 g Pluronic®, and the organic phase contained 50 ml acetone, 0.20 g PCL polymer, and 0.10 g of the previously extracted flaxseed oil.

The aqueous phase was immediately subjected to magnetic stirring. Regarding the organic phase, the oil was initially solubilized in acetone using an ultrasonic

tip sonicator for one minute with 40% power and a 4 mm micro tip. Then the polymer was added, and the solution was kept under magnetic stirring until solubilization of the PCL.

The next step is the nanoprecipitation, the organic solution was poured into the aqueous solution using a glass funnel for liquid in a continuous way. In the end, the emulsion was kept for three days under magnetic stirring at room temperature to the solvent evaporation. After this period, the sample was taken to the freezer for 6 hours at −62˚C and finally to the lyophilizer under the pressure of 2000 μHg and −47˚C. The methodology used in this project was adapted from the literature [18].

2.4. Characterization

2.4.1. Fourier-Transform Infrared Spectroscopy (FTIR)

FTRI was performed with a PerkinElmer Frontier FTIR/FIR spectrometer using KBr pellets at room temperature. The spectra were collected from 4000 to 400 cm^{-1} with a resolution of 4 cm^{-1} and 20 scans.

2.4.2. Nuclear Magnetic Resonance Spectroscopy (NMR)

To obtain the NMR spectra, a Varian Mercury VX 300, 5 mm Universal probe with gradient, operating at a frequency of 300 MHz (for the hydrogen nucleus) was used; the samples were analyzed at a temperature of 30˚C in deuterated chloroform as solvent and reference.

Conditions to Acquire the ^{1}H Spectra

The conditions used to obtain the ^{1}H NMR spectrum were: spectral window equal to 4800 Hz, acquisition time of 2.5; interval between pulses equal to 20 s; number of transients equal to 16 and the pulse calibrated to 90 degrees.

Conditions to Acquire the ^{13}C Spectra

The conditions to obtain the ^{13}C NMR spectrum were: spectral window of 16,600 Hz was used, acquisition time equal to 0.9; interval between pulses equal to 2; number of transients of 3600; pulse calibrated for 90 degrees at a frequency of 75.4 Hz. For the APT (attached proton test), the parameters were similar, except for the acquisition time equal to 0.8; interval between pulses equal to 1 and number of transients equal to 4000.

2.4.3. Time-Domain Unclear Magnetic Resonance (TD-NMR)

After encapsulation, the solid samples were subjected to time-domain nuclear magnetic resonance (TD-NMR) analysis. To determine the nuclear relaxation measurements, a Maran Ultra 23 apparatus was used, operating at 0.54 T (23.4 MHz for $_{1}H$) and equipped with an 18 mm probe, at 30˚C. Two pulse sequences were applied as follows:

MSE-FID Pulse Sequence

To obtain hydrogen signals from the sample phases, the MSE-FID pulse sequence (Magic-sandwich Echo with free induction decay) was applied, using the parameters: 90˚ pulse (duration 7.5 μs), number of 2048 points, interval between each point of 1 μs, number of stacks equal to 32, recycle time of 1 s and receiver gain of 28%.

Inversion-Recovery Pulse Sequence

The hydrogen spin-lattice relaxation time was directly determined by the inversion-recovery pulse sequence (180˚-t-90˚), and the 90˚ pulse (duration 7.5 μs) was automatically calibrated by the equipment's software. The FID amplitude was 40 points ranging from 0.1 to 5000 ms, with 4 measurements for each point with a recycle interval of 1 second.

2.4.4. X-Ray Diffraction (XRD)

XRD analyzes were performed using a Shimadzu LabX XRD-6100 apparatus. The samples were exposed to CuK α radiation (λ = 1.5418 Å) at room temperature and the data were collected from 10˚ to 60˚ degrees theta (2θ) at a scan rate of 0.02˚/s. The degree of crystallinity was calculated using Fityk software and Equation (1), in which the total area is the sum of the crystalline phase and the amorphous phase.

$$Xc = \frac{\text{Cristalline phase area}}{\text{Total area}} \times 100 \quad (1)$$

3. Results

3.1. Characterization of Flaxseed Oil from NMR

The magnetic resonance spectra for the extractions in the different solvents used were obtained, however, they all presented the same signal profile. Thus, only the results obtained for one of the extractions will be presented. Along with NMR, FTIR and the study of the literature are going to be used [19] [20] [21].

Figure 1 presents the ^{1}H spectrum for brown flaxseed oil extracted in ethyl acetate/ethanol (3:1) and Table 1 lists each signal obtained in the spectrum with its chemical shift.

Table 1. Chemical shift of every signals present in the 1H spectrum of flaxseed oil.

Signal	δ (ppm)	Proton type	Components[2]
A	0.86 - 0.91	C**H**$_3$	All acids except linolenic acid
B	0.95 - 1.00	C**H**$_3$	linolenic acid
C	1.26 - 1.31	-(C**H**$_2$)$_n$-	All fatty acids
D	1.59 - 1.63	-C**H**$_2$-CH$_2$-OCO-	All fatty acids
E	2.04 - 2.08	-C**H**$_2$-CH=CH	All unsaturated fatty acids
F	2.28 - 2.34	-C**H**$_2$-OCO-	All fatty acids
G	2.75 - 2.82	-CH=CH-C**H**$_2$-CH=CH-	Linolenic acid and linoleic acid
H	4.12 - 4.33	-C**H**$_2$OCOR	Glycerol
I	5.20 - 5.26[1]	>C**H**OCOR	Glycerol
J	5.24 - 5.37	-C**H**=C**H**-	All unsaturated fatty acids

[1][20]; [2][19].

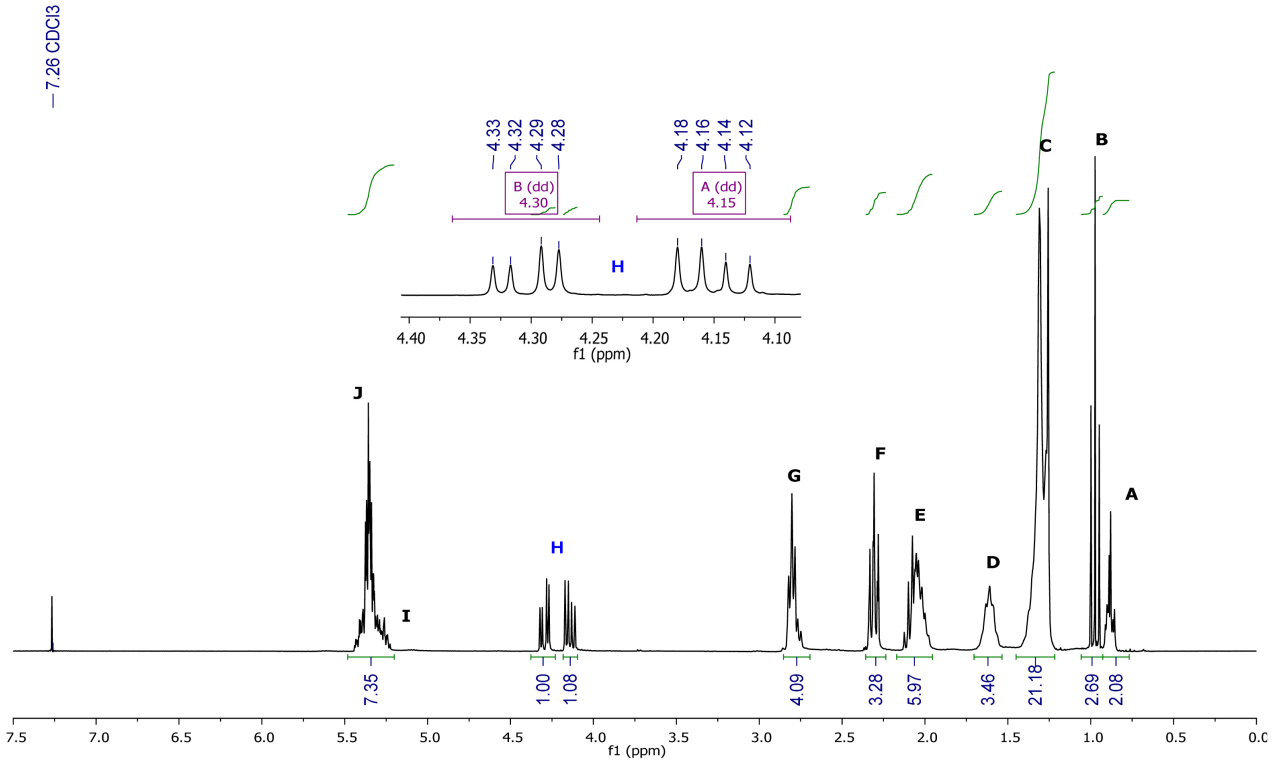

Figure 1. ^{1}H solution NMR spectrum of flaxseed oil.

The data obtained from the hydrogen and carbon spectra as well as the literature data indicate that there is a mixture of fatty acid esters bonded to the three carbons of glycerol [19] as shown in **Figure 2**. The carbons 1 and 3 of the glycerol are linked to the same or very similar molecules, which keeps the symmetry in the molecule.

In the ^{1}H NMR spectrum, two methyl signals can be highlighted, one referring to the *α*-linolenic acid ester (signal B) and the other of the other esters including linoleic acid (signal A), the methyl B signal is more deshielded due to its proximity to a double bond which does not occur with signal A.

Another important sign is the doublet of doublets at the center (H sign) this refers to the hydrogens of the CH_2 groups present in glycerol. The signs C, D, E, F, and G refer to the CH_2 groups present in the chain of these esters, with F being the hydrogens closest to the carbonyl and G being those located between the double bonds, the sign J represents the hydrogens of the double bonds. The description of these signals is summarized in **Table 1**.

In addition to the ^{1}H spectrum, the ^{13}C and APT spectra were obtained (**Figure 3** and **Figure 4**, respectively). The APT spectrum is an important tool to distinguish the types of carbons present, it is possible to observe the methyl groups and CH groups in an inverted way on the spectrum and thus discriminate them from the CH_2 groups and carbons that do not have hydrogen bonded.

In these spectra, it is possible to observe that there are two signals referring to a glycerol molecule. The first at 62.62 ppm for CH_2 and the second at 69.68 ppm

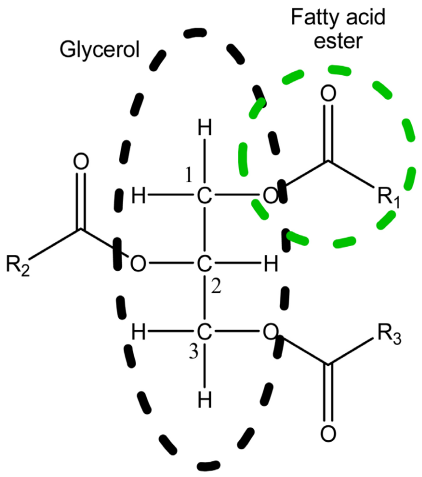

Figure 2. Triglyceride present in the flaxseed oil.

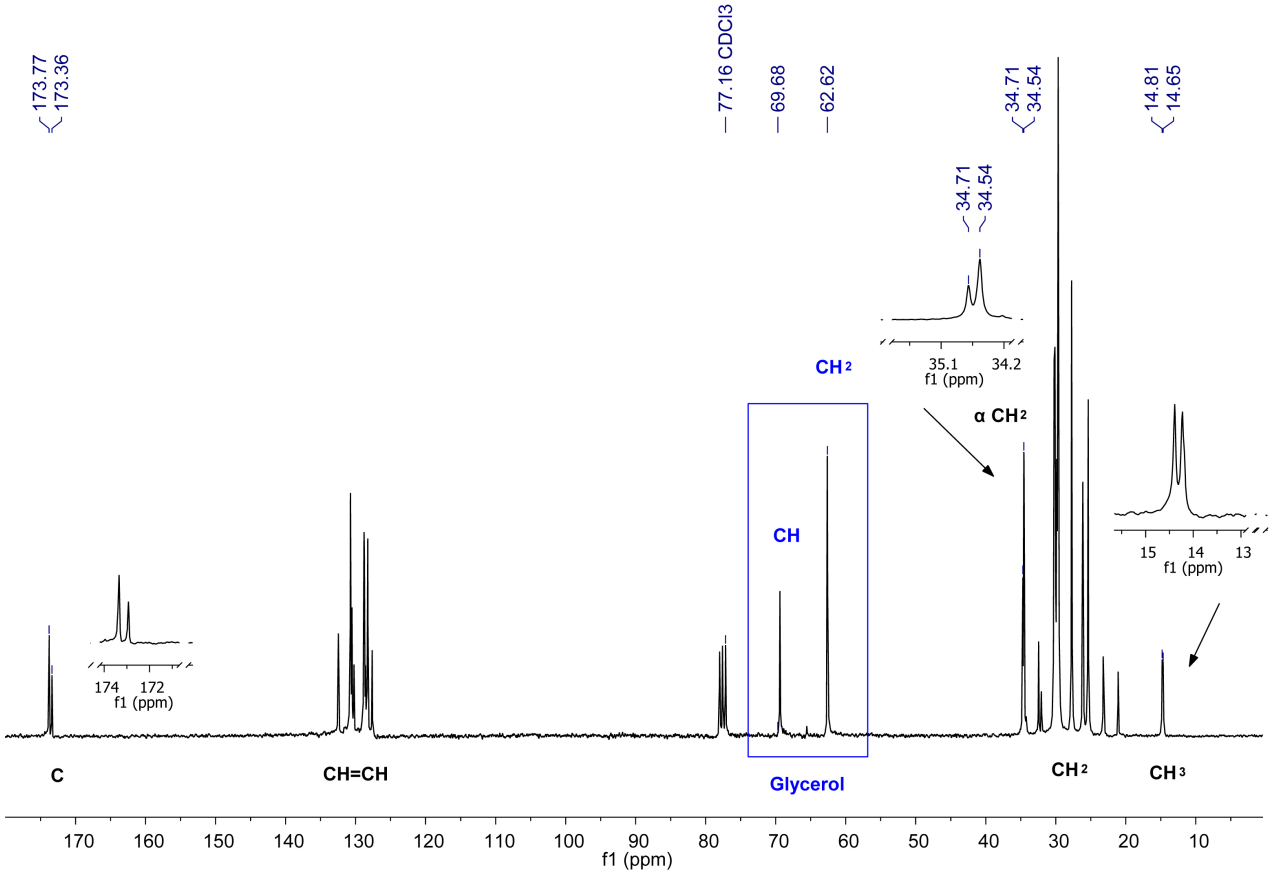

Figure 3. ^{13}C spectrum of flaxseed oil.

for CH, this can be explained by the symmetry of the molecule, causing the two CH_2 signals to fall into the same chemical shift. This issue is reinforced by the signs of the ester carbonyls at 173.36 ppm and 173.77 ppm, the methyls (CH_3) at 14.65 ppm and 14.81 ppm and the *α* CH_2 at 34.54 ppm and 34.71 ppm which has, as can be seen in the enlargements, two signs each (**Figure 3**).

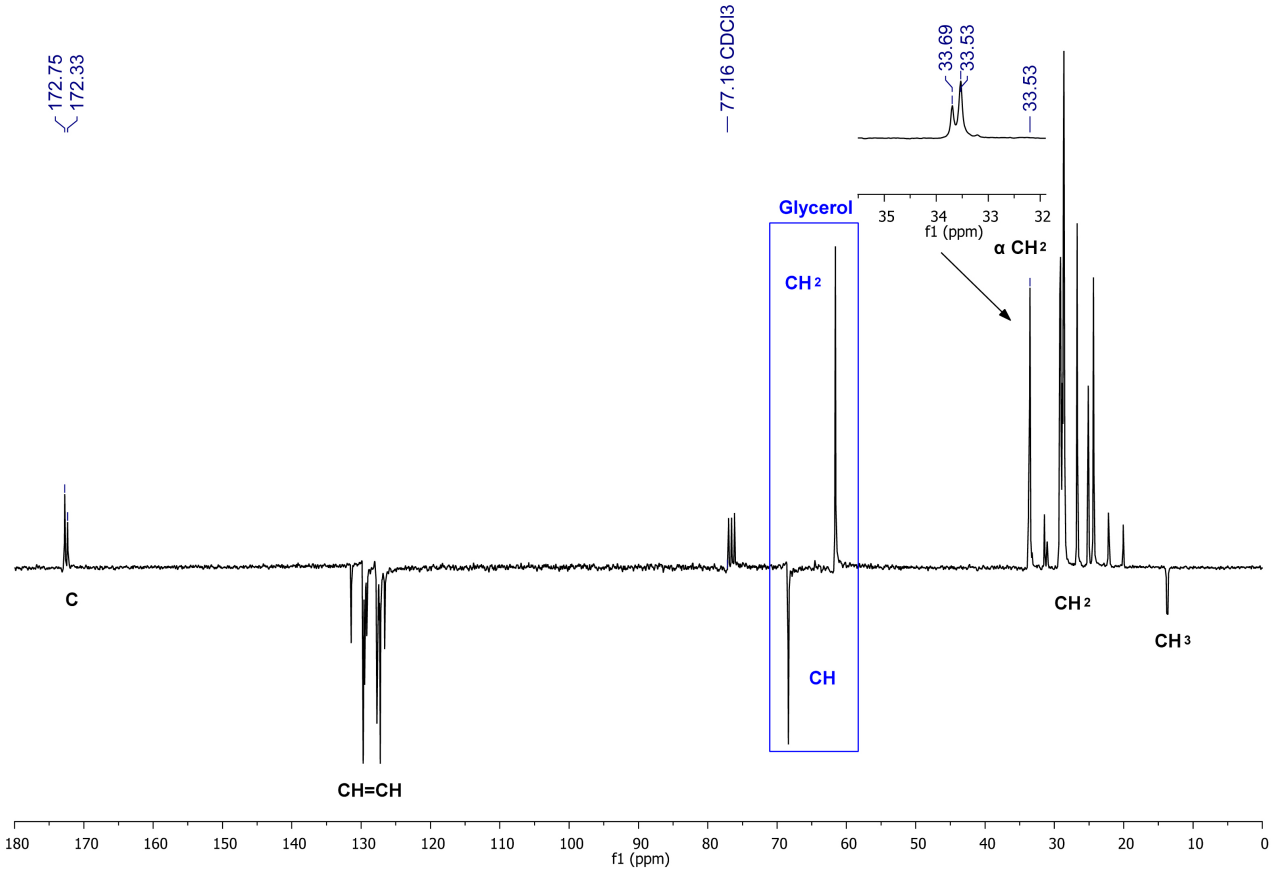

Figure 4. APT spectrum of flaxseed oil.

In order to aid the characterization of the flaxseed oil, the HSQC (Single Quantum Coherence Spectroscopy) and COSY (Correlation Spectroscopy) spectra were also obtained, **Figure 5** and **Figure 6** show these spectra. The first spectrum correlates the hydrogen signals with the carbons which are directly bonded and the second correlates ^{1}H signals with other ^{1}H signals up to three bonds, therefore on adjacent carbons.

In the first part of the spectrum (signals from A to G in the ^{1}H phase), it is possible to observe that these are the hydrogens present in CH_3 and CH_2 correlated with their respective carbons. The most notable of these correlations is between the hydrogens and carbons of the methyls (signals A and B in the ^{1}H spectrum) and the ^{1}H α with α carbon (F signal) as shown in **Figure 5**.

In the second part of the spectrum, the doublet of doublets can be observed at the center of the spectrum (signal H), in the hydrogen phase, these signals can be correlated with the CH_2 carbons of glycerol. Signal I refers to the central hydrogen of glycerol and although it is overlap on sign J, it is possible to see its correlation with the respective carbon. Guillén and Uriarte (2012) described this CH hydrogen signal around 5.20 to 5.26 as shown in **Table 1**.

Finally, the third part of the spectrum shows the correlations between the unsaturation hydrogens (signal J) with their carbons. The last signal that appears in

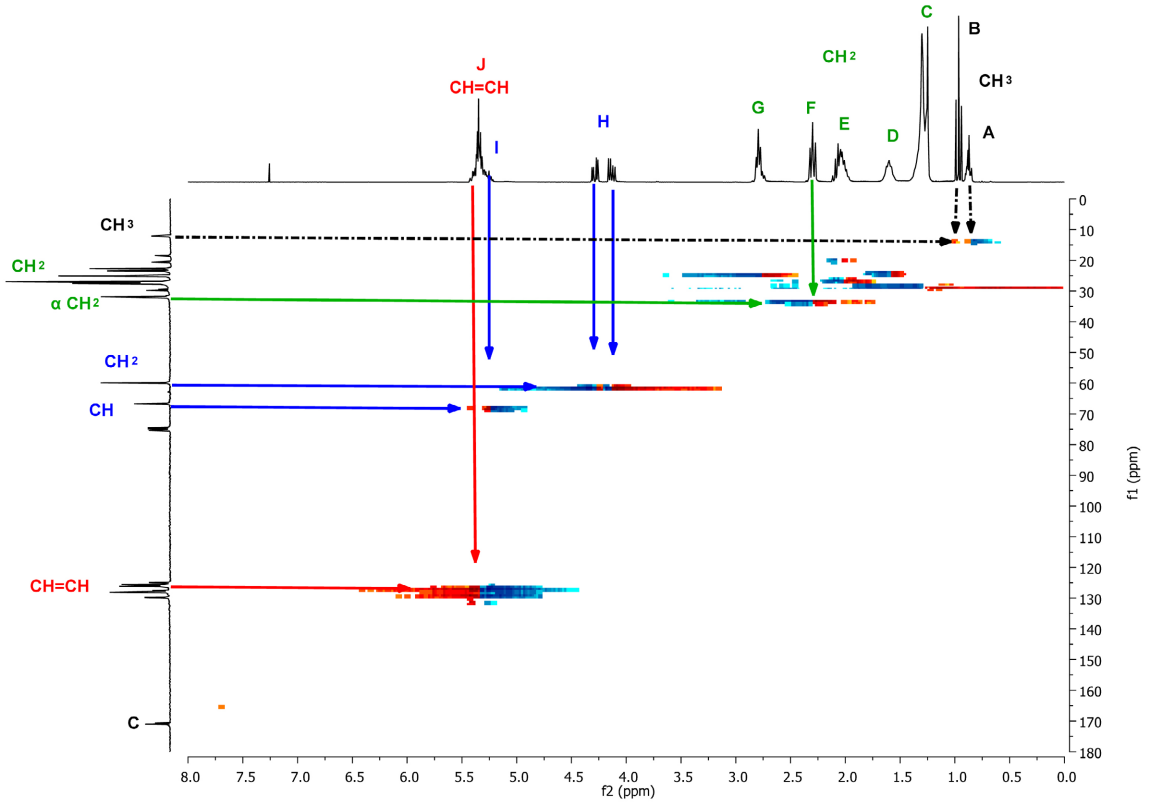

Figure 5. HSQC spectrum of flaxseed oil.

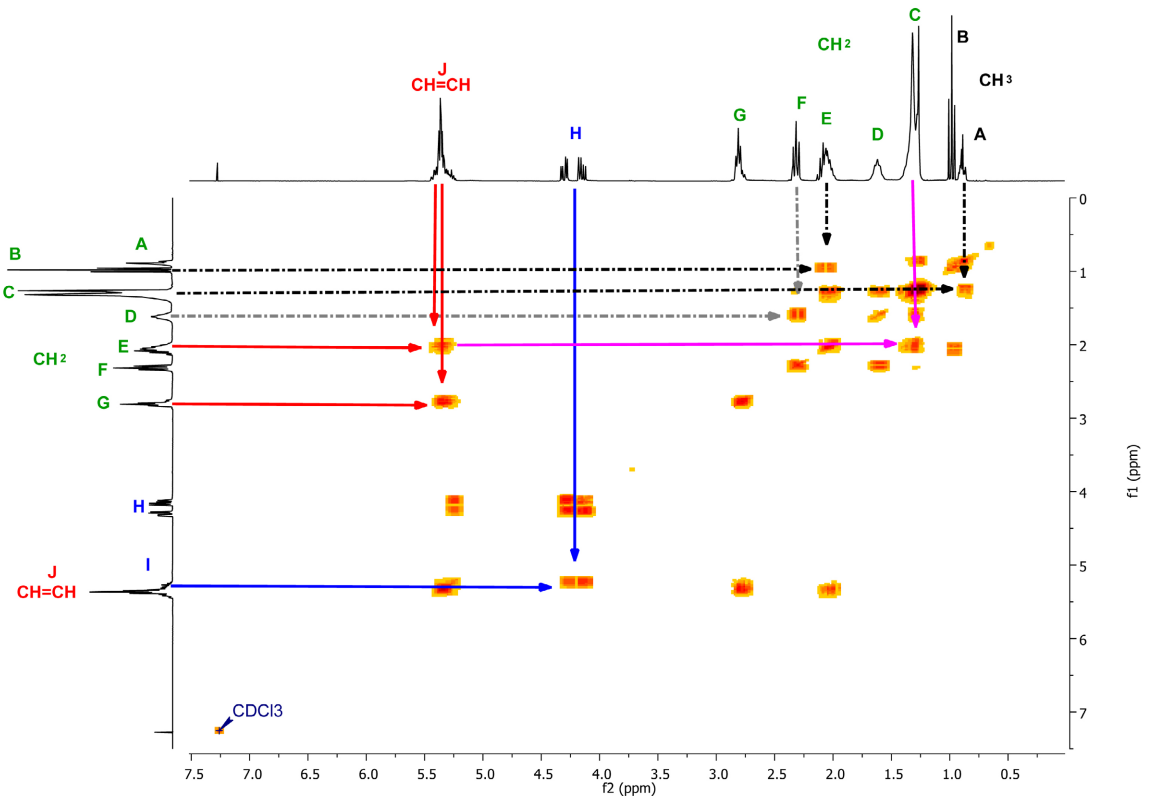

Figure 6. COSY spectrum of flaxseed oil.

the carbon phase, in which there is no correlation on the spectrum is the carbons of the ester carbonyls, this signal is also doubled in the enlargement of the 13C spectrum.

Regarding the COSY spectrum (Figure 6) in the first part, it is possible to highlight the methyl A signals with the CH_2 groups that are not close to the unsaturation (C signal), this last signal also correlates to the E signal that refers to neighboring hydrogens of the double bonds (pink arrows on the spectrum). The E signal correlates with the B in the case of the *α*-linolenic acid ester molecule due to unsaturation near the chain ends.

It is also possible to observe the correlation between the F and D signals, respectively, the *α* and *β* hydrogens of the esters chain. Then we have the correlation between H and I (overlapped on the J signal), that is, the hydrogens of the CH_2 groups of the glycerol with its central hydrogen. Finally, it is possible to correlate the J signal (^1H of the unsaturation) with the signals G and E CH_2 near the unsaturation carbons. Table 2 summarizes all the signals handled so far.

3.2. Characterization of Flaxseed Oil by FTIR

The FTIR analysis confirms the presence of unsaturated fatty acid ester due to the presence of bands of 3010 cm^{-1}, 1739 cm^{-1}, 1647 cm^{-1} and 1242 cm^{-1}, these and the other bands are also reported in other research such as in Bălănucă *et al.* (2014). The band at 1739 cm^{-1} refers to the stretching of the ester carbonyl and the band at 1242 cm^{-1} to the stretching of the CO bond. Moreover, the bands at 3010 cm^{-1} and 1647 cm^{-1} are attributed to the double bonds present in the chains as can be seen in Table 3 and Figure 7.

3.3. Dynamic Light Scattering (DLS)

DLS technique was performed aiming to determine particle size and polydispersity (PDI) after the oil encapsulation. Table 4 shows the mean diameter size and PDI values for the analysis performed at the end of lyophilization.

The mean diameter obtained in the analysis indicates that the particles formed are microparticles. The PDI indicates the homogeneity of the system in relation

Table 2. Summary of correlations presented in the solution spectra.

Correlations	Signals
D e F	*β* CH_2 e *α* CH_2
E e C	CH_2-CH=CH e CH_2 (others)
J e G	CH=CH e CH=CH-CH_2-CH=CH
J e E	CH=CH e CH_2-CH=CH
B e E	CH_3 e CH_2-CH=CH
A e C	CH_3 e CH_2 (others)
I e H	CH (Glycerol) e CH_2 (Glycerol)

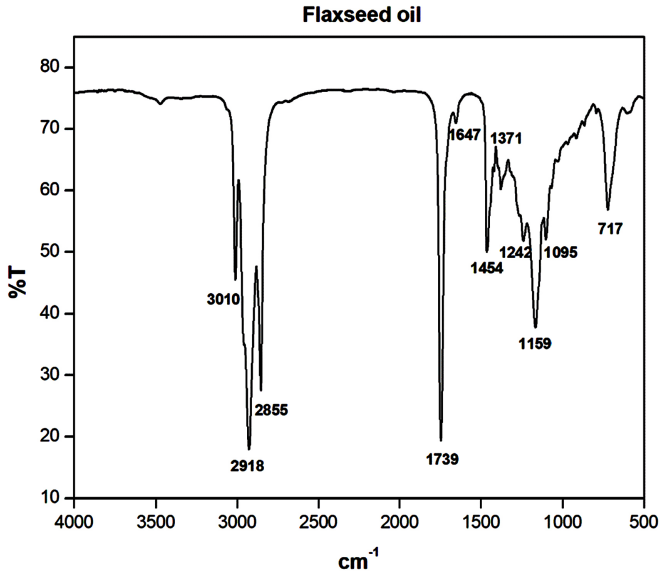

Figure 7. FTIR spectrum of flaxseed oil.

Table 3. Wavelength of functional groups present in flaxseed (in cm^{-1}).

Flaxseed oil (cm^{-1})	Groups	Flaxseed oil (cm^{-1})	Groups
3010	ν=CH-	**1371**	δCH_3
2918	νC-H assimétrica	**1242**	νC-O
2855	νC-H simétrica	**1159**	νC-O
1739	νC=O	**1095**	νC-O
1647	νC=C	**717**	ρCH_2
1454	δCH_2	-	-

Table 4. Mean diameter and PDI of the sample.

Time	Mean diameter (nm)	PDI
Initial sample	445.2 ± 41	0.674 ± 0.064

to the particle size distribution. Thus, the smaller the PDI value, the more monodisperse the sample (this value varies between 0 and 1).

In this way, for the analysis in question, it is possible to observe that the material after encapsulation has a wider size distribution, which may be due to the collapse of the sample during the solidification and lyophilization processes [18].

During the freeze-drying process, also called lyophilization, there was an oscillation of pressure and temperature during the sublimation of the solvent, causing the sample to be solidified again in the freezer. Furthermore, a cryoprotectant was not used, so some particles may have agglomerated and reorganized, generating a mean diameter with a high standard deviation and a polydispersity around 0.674 indicating a greater polydispersion, however for this methodology

there are cases in the literature with better results such as Tavares *et al.* (2017).

Thus, even with the problems faced, the project obtained PCL microparticles through the nanoprecipitation process, but it is important to have greater control over the parameters, especially in the freeze-drying step.

3.4. X-Ray Diffraction Analysis of the Encapsulated Material

The X-ray diffraction analyses for the analyzed materials were obtained in the 2θ range between 10˚ and 60˚, as outside this range, no significant diffraction maxima were observed for the analyzed polymers or for the sample after encapsulation. Table 5 shows the angles obtained in the analyses performed.

Figure 8 shows the diffractogram of pure PCL, it is possible to observe the diffraction maxima of this polymer at 2θ = 21.7˚ and 23.9˚, this is due to the semi-crystalline structure of this polymer and corresponds to the diffraction maxima described in the literature, corresponding to the planes (110) and (200) of the orthorhombic crystal structure, respectively [22]. Other diffraction maxima can also be observed above 2θ = 30˚, these correspond to less important crystalline domains of the polymer used in the analysis.

In relation to Pluronic® F-68 (Figure 9), diffraction maxima at 2θ = 19.4˚ and 23.4˚ were observed, also similar to those observed in the literature [23].

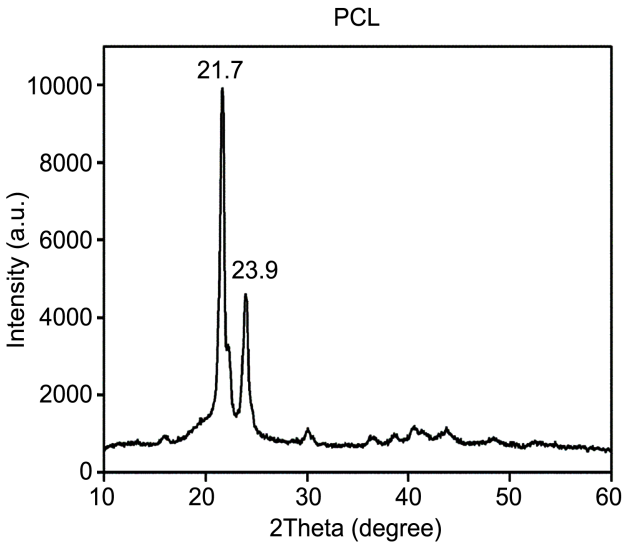

Figure 8. PCL diffractogram.

Table 5. Diffraction maxima and crystalinity of the analyzed materials.

Materials	Diffraction máxima (˚)			Crystalinity (%)
PCL	21.7	-	23.9	30%
Pluronic® F-68	19.4	-	23.4	18%
Encapsulated material	20.4	22.6	24.8	27%

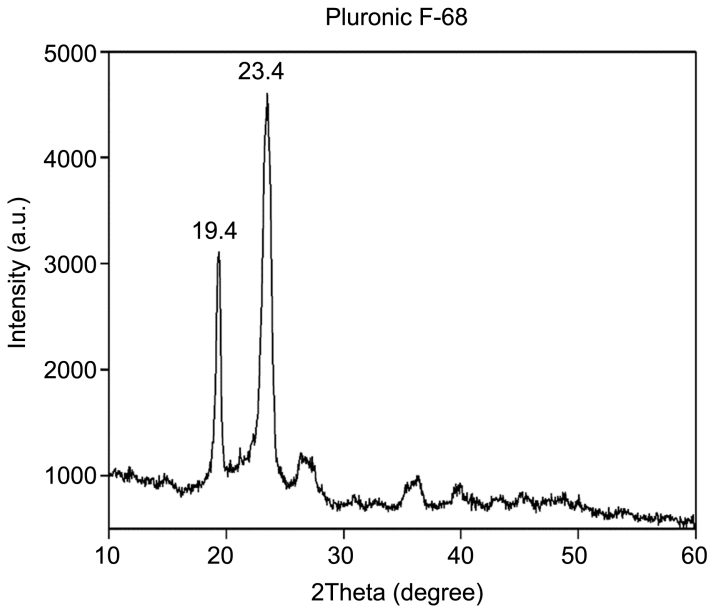

Figure 9. Pluronic® diffractogram.

Regarding the material after encapsulation, in **Figure 10**, the sample showed three diffraction maxima, at $2\theta = 20.4^{\circ}$, 22.6°, and 24.8°. The first may be associated with Pluronic® F-68, the second with PCL polymer, and the third with an overlap of the PCL and Pluronic® F-68 diffraction maxima.

Another factor to be considered is that during the analyses, it was necessary to press the material into the sample holder, which caused it to change its visual appearance, that is, it was no longer a white powder and became a more compact mass that is difficult to be worked on and with slightly different coloration, this suggests that at that time there was an oil release and this, as well as Pluronic® F-68, affected the crystallinity of the PCL. This can be highlighted when calculating the degree of crystallinity of the polymers and the sample, the PCL had 30% crystallinity, the Pluronic® F-68 18%, and the sample 27%. Thus, the oil reduced the crystallinity of the PCL in the sample.

3.5. MSE-FID Analysis

In order to confirm whether or not the oil was encapsulated, pulse sequences MSE-FID (Magic-sandwich echo-Free induction decay) were used. The data of the material after encapsulation, PCL, and Pluronic® F-68 can be analyzed in **Table 6**.

In the MSE-FID sequence, a longer T_2^* time indicates greater mobility of the phase in question. Then, using the data in **Table 6**, it can be stated that the flaxseed oil was encapsulated since the sample presented an increase in time T_2^* compared to the PCL values, this means that there was an increase in the mobility of the phases, an indication that the oil was encapsulated. This increase can also be observed when comparing the T_2^* of the intermediary and rigid phases of Pluronic® and the material after encapsulation.

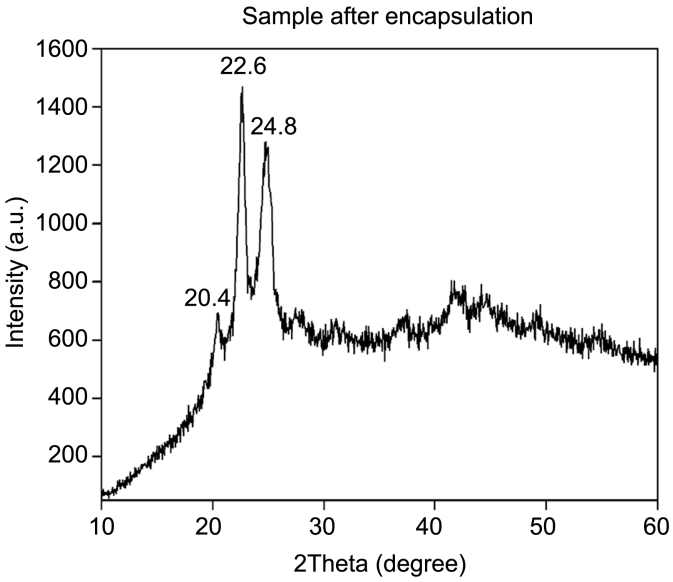

Figure 10. Diffractogram of encapsulated material.

Table 6. Spin-spin relaxation time (T_2H) attributed to rigid ($T_{2r}H$), intermediary ($T_{2i}H$) and mobile ($T_{2m}H$) domains for polymer, Pluronic®, and Encapsulated material (in μs).

Sample	$T_{2r}H$	$T_{2i}H$	$T_{2m}H$
PCL	14	94	230
Pluronic®	33	124	307
Encapsulated material	17	141	358

3.6. FTIR Analysis of Encapsulated Material

Besides the MSE-FID sequence, the FTIR technique was also used to confirm that the oil was encapsulated. Figure 11 shows the FTIR spectrum of the material after encapsulation, in this spectrum, there are bands similar to those of the PCL polymer. Nevertheless, the bands of Pluronic® F-68 and the characteristic bands of the oil are not observed thus being another indication that the flaxseed oil was encapsulated.

In the microencapsulate, the band at 3444 cm^{-1} is observed, similar to that present in the PCL spectrum. Moreover, the ester band at 1730 cm^{-1} is characteristic of the polymer, remembering that in the oil spectrum there is also a band of the same type, but in 1739 cm^{-1}.

In addition to these bands those that occur in 1288 cm^{-1}, 1242 cm^{-1}, and 1177 cm^{-1} stand out, these are also polymer bands, since they do not resemble the flaxseed oil ones that occur in the same region, but with those that are present in the PCL spectrum.

3.7. Analyses of Flaxseed Flour from TD-NMR

3.7.1. Inversion-Recovery

Figure 12 shows the distribution graphs of longitudinal relaxation domains (T_1)

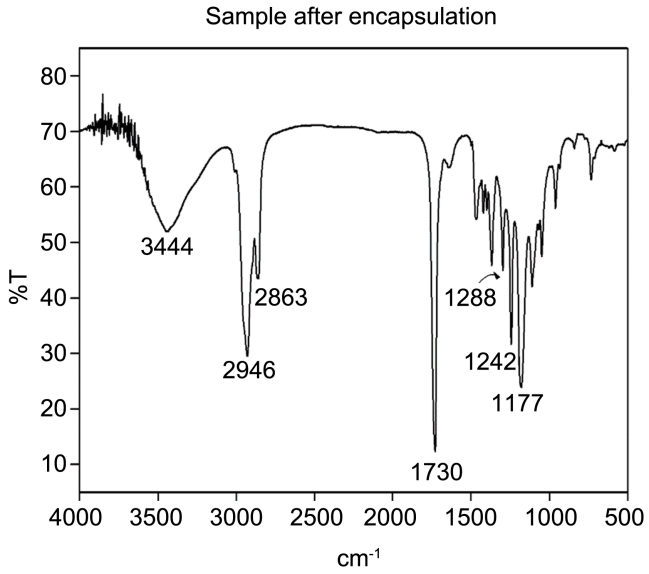

Figure 11. FTIR spectrum of material after encapsulation.

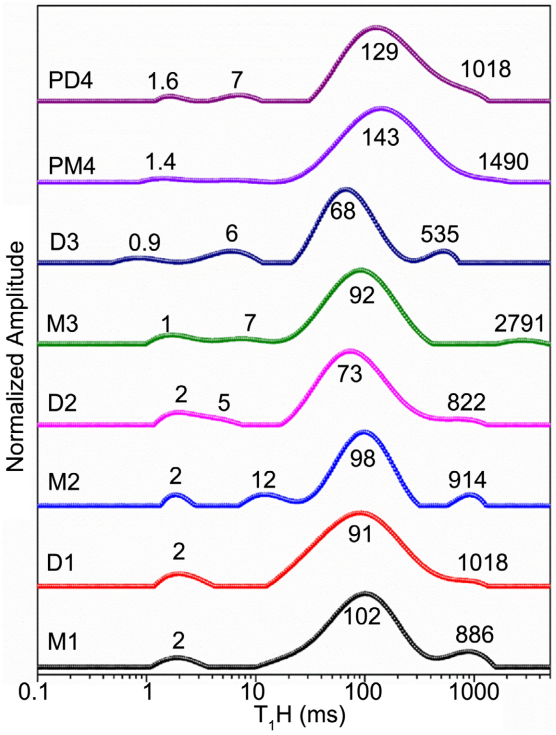

M1: Brown flaxseed in ethanol; **D1:** Golden flaxseed in ethanol; **M2:** Brown flaxseed in chloroform; **D2:** golden flaxseed in chloroform; **M3:** Brown flaxseed in ethyl acetate/ethanol; **D3:** Golden flaxseed in ethyl acetate/ethanol; **PM4:** Brown flaxseedstandard; **PD4:** Golden flaxseed standard.

Figure 12. Distribution curves of domain relaxation times for flaxseed flour.

obtained by inversion-recovery for brown and golden flaxseed flour after extraction in the solvents ethanol, chloroform, and ethyl acetate/ethanol (3:1), and flaxseed flours before the extraction.

In these graphs and in Table 7 and Table 8, it is possible to observe that the solvents had a significant effect on the extractions, influencing the composition of the residual material since there are differences in the T_1 relaxation time values of the standard materials (PM4 and PD4) and materials after extractions (M1, D1, M2, D2, M3, D3). These variations may be due to the interactions that these bioactive make with other components of the rigid phase. It is important to emphasize that the shorter the T_1 relaxation time, the greater the molecular mobility of the chains and the weaker the interactions between the components of this phase.

Thus, it can be emphasized that some samples of brown flaxseed flour showed a smaller variation in the T_1 relaxation time values compared to the values of the golden flaxseed. In Table 7 and Figure 12, it is possible to notice that the most efficient extractions of brown flaxseed are M2 and M3 due to a greater reduction in T_1 when compared to the standard.

With regard to the golden flaxseed (Table 8), this showed better efficiency in the D3 extraction, because, as it can be seen, in addition to the significant reduction in T_1 in relation to its standard, there was also a reduction in the curve of the graph (third curve in the graph).

The width of the relaxation domain curves is an important point, as the wider the more heterogeneous the phase is. The phase has hydrogen nuclei with distinct molecular mobility and interactions. Thus, the greater decrease in the width of the curves of the golden flaxseed indicates a greater structural reorganization of the phases after the extraction of the bioactive, making the phase more

Table 7. Spin-lattice relaxation time (T_1H) for brown flaxseed flour (in ms). PM4: Standard; M1: flaxseed in ethanol; M2: flaxseed in chloroform; M3: flaxseed in ethyl acetate/ethanol.

Sample	T_1H of Brown Flaxseed (ms)			
PM4	1.4	-	143	1490
M1	2	-	102	886
M2	2	12	98	914
M3	1	7	92	2791

Table 8. Spin-lattice relaxation time (T_1H) for golden flaxseed flour (in ms). PD4: Standard; D1: flaxseed in ethanol; D2: flaxseed in chloroform; D3: flaxseed in ethyl acetate/ethanol.

Sample	T_1H of Golden Flaxseed (ms)			
PD4	1.6	7	129	1018
D1	2	-	91	1018
D2	2	5	73	822
D3	0.9	6	68	535

homogeneous in the more rigid phase (the one with the highest T_1), especially when the extraction was carried out with the ethyl acetate/ethanol mixture (D3) and the solvent chloroform (D2). The same happened in relation to brown flaxseed, which presented a more prominent curve variation in chloroform (M2) and ethyl acetate/ethanol (M3).

Therefore, the extraction of golden flaxseed using ethyl acetate/ethanol (D3) was the one with the highest extraction power, since there was a significant decrease in the relaxation time (T_1) and a decrease in the width of the curves, indicating that after extraction the phase became a little more homogeneous compared to standard flaxseed (PD4). The extractions of brown flaxseed were a little less efficient compared to golden flaxseed, but the efficiency of the ethyl acetate/ethanol system (3:1) can be highlighted again.

3.7.2. MSE-FID Analyses of Flaxseed Flour

Regarding the MSE-FID analysis, this measures the relaxation time T_2^* (transverse relaxation time), the behavior of T_2^* is the opposite of T_1, that is, a phase or domain with a high T_2^* value is a phase with less molecular mobility.

Through Table 9, it can be seen that the T_2^* of the rigid phase varied randomly, for the brown flaxseed, which may be due to the strength of solvent interaction. Regarding the mobile phase, this showed a noticeable difference for samples M2 and M3, respectively 281 μs and 283 μs (Table 9) compared to the standard value (PM4) of 712 μs that is, the mobility of the phase decreased.

The M1 sample, with T_2^* of 612 μs for the mobile phase, showed the least variation compared to the standard (PM4) which may indicate and corroborate the effect of the solvent action in the extraction, being similar to samples M2 and M3 and different from sample M1. The same behavior was observed for the intermediary domain. These results agree with the results presented by the inversion-recovery pulse sequence in which the M2 and M3 samples had a shorter T_1H time compared to the M1 extraction and the standard.

Thus, it can be stated that the mixture of ethyl acetate/ethanol (3:1) and the solvent chloroform were the most efficient for the extraction of brown flaxseed flour.

For golden flaxseed flour, the rigid domain showed little or no variation when compared to the standard of 16 μs. For the mobile and intermediary phases, there was a reduction in the relaxation time in the D1 and D3 extractions indicating that these phases lost mobility after the extraction. On the other hand, the D2 extraction (chloroform extraction) presented an increase in the T_2^* time which means that the hydrogens in this phase have even more mobility after the procedure which is indicative of a system reorganization (Table 10).

These results are in part in agreement with the results presented by the inversion-recovery pulse sequence, as this showed better extraction efficiency for the ethyl acetate/ethanol (3:1) mixture. The same occurs for the MSE-FID pulse sequence since the D3 extraction was the one with the smallest T_2^*. The golden flaxseed D1 (ethanol) also showed a good result, but even so the most efficient is D3.

Table 9. Spin-spin relaxation time (T_2H) attributed to rigid ($T_{2r}H$), intermediary ($T_{2i}H$) and mobile ($T_{2m}H$) domains for brown flaxseed flour (in μs). PM4: Standard; M1: flaxseed in ethanol; M2: flaxseed in chloroform; M3: flaxseed in ethyl acetate/ethanol.

Sample	$T_{2r}H$	$T_{2i}H$	$T_{2m}H$
PM4	24	162	712
M1	13	167	612
M2	21	119	281
M3	15	114	283

Table 10. Spin-spin relaxation time (T_2H) attributed to rigid ($T_{2r}H$), intermediary ($T_{2i}H$), high mobile ($T_{2hm}H$), and mobile ($T_{2m}H$) domains for brown flaxseed flour (in μs). PD4: Standard; D1: flaxseed in ethanol; D2: flaxseed in chloroform; D3: flaxseed in ethyl acetate/ethanol.

Sample	$T_{2r}H$	$T_{2i}H$	$T_{2m}H$	$T_{2hm}H$
PD4	16	158	458	993
D1	16	144	414	-
D2	14	174	489	-
D3	15	128	367	-

Another important point is that the golden flaxseed without extraction presented a domain with high mobility hydrogens (993 μs), this phase was not observed in the other analyses of the golden or brown flaxseed. The disappearance of this phase after the extraction is an indication that the extractions were efficient, removing the highly mobile hydrogens and that the system reorganized and the remaining molecules started to interact more with each other in this phase, making it less mobile.

4. Conclusions

In this project, the flaxseed oil was extracted and characterized using FTIR and NMR and the results compared with the literature, it can be concluded that the oil contains fatty acid esters in the form of triglycerides, in which there is the presence of ALA and LA, respectively, the *α*-linolenic and linoleic acid esters an omega 3 and 6.

After the characterization, the encapsulation of the oil was carried out using the nanoprecipitation technique followed by lyophilization to obtain PCL microcapsules. The DLS results showed that there was the formation of microparticles with a mean diameter of 445.2 ± 41 nm and PDI of 0.674 ± 0.064. During freeze-drying, there were some problems that affected the formation of these microparticles, which highlights the importance of controlling the temperature and the pressure during this step.

The XRD analyses of the encapsulated material showed a sightly change in the

diffraction maxima. Nonetheless, the diffraction maxima of the sample can be associated with the Pluronic® F68 and the PCL. Moreover, its crystallinity is lower than the polymer which may be due to the oil released during the preparation of the analysis.

In order to confirm that the oil was encapsulated, the pulse sequence MSE-FID and the FTIR were used, the first one showed that there was an increase in the T_2* time of the sample in relation to the polymer and the surfactant used, which indicates high molecular mobility of the phases provided by the oil, an indicative of encapsulation. The second technique used also reinforces this issue since it is not possible to observe characteristic bands of the oil in the FTIR spectrum of the sample.

This project also analyzed the flaxseed flour obtained as residue from the extractions. The results of TD-NMR using two types of pulse sequence: inversion-recovery and MSE-FID agree with each other showing that the most efficient solvent was the mixture of ethyl acetate/ethanol (3:1) for both types of flaxseed.

Therefore, it can be concluded that flaxseed oil was encapsulated in PCL, a biodegradable and biocompatible polymer. The particles are in the micrometric scale, making it ideal for application in the food and nutraceuticals area due to the documented benefits of flaxseed oil for human health. The nanoprecipitation technique can also be used in other areas such as cosmetics and pharmacology encapsulating different types of materials.

Acknowledgements

We acknowledge CNPq and FAPERJ and CAPES Code 001 for the support of this work.

Conflicts of Interest

The authors declare no conflicts of interest regarding the publication of this paper.

References

[1] Kaur, P., Waghmare, R., Kumar, V., Rasane, P., Kaur, S. and Gat, Y. (2018) Recent Advances in Utilization of Flaxseed as Potential Source for Value Addition. *Oilseeds and Fats, Crops and Lipids*, **25**, Article No. A304. https://doi.org/10.1051/ocl/2018018

[2] Goyal, A., Sharma, V., Upadhyay, N., Gill, S. and Sihag, M. (2014) Flax and Flaxseed Oil: An Ancient Medicine & Modern Functional Food. *Journal of Food Science and Technology*, **51**, 1633-1653. https://doi.org/10.1007/s13197-013-1247-9

[3] Kajla, P., Sharma, A. and Sood, D.R. (2015) Flaxseed—A Potential Functional Food Source. *Journal of Food Science and Technology*, **52**, 1857-1871. https://doi.org/10.1007/s13197-014-1293-y

[4] Sweazea, K.L. and Johnston, C.S. (2019) Chapter 24. Cardioprotective Potential of Flaxseeds in Diabetes. In: Watson, R.R. and Preedy, V.R., Eds., *Bioactive Food as Dietary Interventions for Diabetes*, 2nd Edition, Academic Press, Reino Unido,

361-374. https://doi.org/10.1016/B978-0-12-813822-9.00024-2

[5] Almehmadi, A., Lightowler, H., Chohan, M. and Clegg, M.E. (2021) The Effect of a Split Portion of Flaxseed on 24-h Blood Glucose Response. *European Journal of Nutrition*, **60**, 1363-1373. https://doi.org/10.1007/s00394-020-02333-x

[6] Edel, A.L., Rodriguez-Leyva, D., Maddaford, T.G., Caligiuri, S.P., Austria, J.A., Weighell, W., *et al.* (2015) Dietary Flaxseed Independently Lowers Circulating Cholesterol and Lowers It beyond the Effects of Cholesterol-Lowering Medications alone in Patients with Peripheral Artery Disease. *The Journal of Nutrition*, **145**, 749-757. https://doi.org/10.3945/jn.114.204594

[7] Katare, C., Saxena, S., Agrawal, S., Prasad, G. and Bisen, P.S. (2012) Flax Seed: A Potential Medicinal Food. *Journal of Nutrition & Food Sciences*, **2**, Article No. 120. https://doi.org/10.4172/2155-9600.1000120

[8] Theegala, M., Arévalo, R.A.C., Viana, V., Olson, D. and Aryana, K. (2021) Effect of Flaxseed on Bile Tolerances of *Lactobacillus acidophilus*, *Lactobacillus bulgaricus*, and *Streptococcus thermophilus*. *Food and Nutrition Sciences*, **12**, 670-680. https://doi.org/10.4236/fns.2021.127050

[9] Liao, W., Badri, W., Dumas, E., Ghnimi, S., Elaissari, A., Saurel, R., *et al.* (2021) Nanoencapsulation of Essential Oils as Natural Food Antimicrobial Agents: An Overview. *Applied Sciences*, **11**, Article No. 5778. https://doi.org/10.3390/app11135778

[10] Pateiro, M., Gómez, B., Munekata, P.E.S., Barba, F.J., Putnik, P., Kovačević, D.B., *et al.* (2021) Nanoencapsulation of Promising Bioactive Compounds to Improve Their Absorption, Stability, Functionality and the Appearance of the Final Food Products. *Molecules*, **26**, Article No. 1547. https://doi.org/10.3390/molecules26061547

[11] Assadpour, E. and Jafari, S.M. (2019) Chapter 3. Nanoencapsulation: Techniques and Developments for Food Applications. In: Rubio, A.L., Rovira, M.J.F., Sanz, M.M. and Mascaraque, L.G., Eds., *Nanomaterials for Food Applications*, Elsevier, Amsterdam, 35-61. https://doi.org/10.1016/B978-0-12-814130-4.00003-8

[12] Jafari, S.M. (2017) An Overview of Nanoencapsulation Techniques and Their Classification. In: Jafari S.M., Ed., *Nanoencapsulation Technologies for the Food and Nutraceutical Industries*, Academic Press, Cambridge, 1-34. https://doi.org/10.1016/B978-0-12-809436-5.00001-X

[13] Yadav, K.S. and Sawant, K.K. (2010) Modified Nanoprecipitation Method for Preparation of Cytarabine-Loaded PLGA Nanoparticles. *AAPS PharmSciTech*, **11**, 1456-1465. https://doi.org/10.1208/s12249-010-9519-4

[14] Barreras-Urbina, C.G., Ramírez-Wong, B., López-Ahumada, G.A., Burruel-Ibarra, S.E., Martínez-Cruz, O., Tapia-Hernández, J.A., *et al.* (2016) Nano and Micro-Particles by Nanoprecipitation: Possible Application in the Food and Agricultural Industries. *International Journal of Food Properties*, **19**, 1912-1923. https://doi.org/10.1080/10942912.2015.1089279

[15] Ezhilarasi, P.N. (2013) Nanoencapsulation Techniques for Food Bioactive Components: A Review. *Food and Bioprocess Technology*, **6**, 628-647. https://doi.org/10.1007/s11947-012-0944-0

[16] Kaliva, M. and Vamvakaki, M. (2020) Chapter 17. Nanomaterials Characterization. In: Narain, R., Ed., *Polymer Science and Nanotechnology*, Elsevier, Amsterdam, 401-433. https://doi.org/10.1016/B978-0-12-816806-6.00017-0

[17] Ikehara, T. and Nishi, T. (2000) Primary and Secondary Crystallization Processes of Poly(ϵ-Caprolactone)/Styrene Oligomer Blends Investigated by Pulsed NMR. *Polymer*, **41**, 7855-7864. https://doi.org/10.1016/S0032-3861(00)00134-8

[18] Tavares, M.R., de Menezes, L.R., Dutra Filho, J.C., Cabral, L.M. and Tavares, M.I.B. (2017) Surface-Coated Polycaprolactone Nanoparticles with Pharmaceutical Application: Structural and Molecular Mobility Evaluation by TD-NMR. *Polymer Testing*, **60**, 39-48. https://doi.org/10.1016/j.polymertesting.2017.01.032

[19] Bălănucă, B., Stan, R., Hanganu, A. and Iovu, H. (2014) Novel Linseed Oil-Based Monomers: Synthesis and Characterization. *University Politehnica of Bucharest Scientific Bulletin*, **76**, 129-140.

[20] Guillén, M.D. and Uriarte, P.S. (2012) Monitoring by 1H Nuclear Magnetic Resonance of the Changes in the Composition of Virgin Linseed Oil Heated at Frying Temperature. Comparison with the Evolution of Other Edible Oils. *Food Control*, **28**, 59-68. https://doi.org/10.1016/j.foodcont.2012.04.024

[21] Nieva-Echevarría, B., Goicoechea, E. and Guillén, M.D. (2017) Behaviour of Non-Oxidized and Oxidized Flaxseed Oils, as Models of Omega-3 Rich Lipids, during *in Vitro* Digestion. Occurrence of Epoxidation Reactions. *Food Research International*, **97**, 104-115. https://doi.org/10.1016/j.foodres.2017.03.047

[22] Yıldırım, S., Demirtaş, T.T., Dinçer, C.A., Yıldız, N. and Karakeçili, A. (2018) Preparation of Polycaprolactone/Graphene Oxide Scaffolds: A Green Route Combining Supercritial CO_2 Technology and Porogen Leaching. *The Journal of Supercritical Fluids*, **133**, 156-162. https://doi.org/10.1016/j.supflu.2017.10.009

[23] Mohamed, E.A., Abu Hashim, I.I., Yusif, R.M., Shaaban, A.A.A., El-Sheakh, A.R., Hamed, M.F., *et al.* (2018) Polymeric Micelles for Potentiated Antiulcer and Anticancer Activities of Naringin. *International Journal of Nanomedicine*, **13**, 1009-1027. https://doi.org/10.2147/IJN.S154325